Generation, propagation and escape of astrophysical cyclotron-maser emission

D. C. Speirs[1], R. Bingham[1,2], R.A. Cairns[3], B.J. Kellett[2], K.M. Gillespie[1], K. Ronald[1], S.L. McConville[1], A.D.R. Phelps[1], I. Vorgul[3] and A.W. Cross[1]

[1]*SUPA, Department of Physics, University of Strathclyde, Glasgow, G4 0NG, U.K.*

[2]*Space Physics Division, STFC Rutherford Appleton Laboratory, Didcot, OX11 0QX, U.K.*

[3]*School of Mathematics and Statistics, University of St Andrews, St Andrews, KY16 9SS, U.K.*

Numerous astrophysical plasma environments exist where a combination of particle acceleration, non-uniform magnetic fields and a sufficiently large ratio of electron cyclotron frequency to plasma frequency are present to support electron cyclotron-maser emission [1]. The resultant radiation signatures typically comprise of well-defined spectral components (around the relativistic electron cyclotron frequency) with near 100% left or right handed circular polarization when viewed out-with the source region. For the planetary auroral case it is now widely accepted that such emissions are generated by an electron cyclotron-maser instability driven by a horseshoe shaped electron velocity distribution [2-5]. Such distributions are formed when particles descend into the increasing magnetic field of planetary auroral magnetospheres, where conservation of magnetic moment results in the conversion of axial momentum into rotational momentum. Theory has shown that such distributions are unstable to cyclotron emission in the X-mode [3] and inhomogeneous systems have also been examined [6]. Given the prevalence of converging magnetic fields in astrophysics it has been suggested that the horseshoe maser can also explain radio emission from stars with a dipole magnetic field [7,8], blazar jets [1,9] and shocks. Although the generation mechanism has been well documented [1-9], there are numerous potential hindrances to the propagation and escape of the radiation from the source region, including second harmonic cyclotron absorption [1] and the obstacle of coupling onto the dispersion branch connecting with vacuum propagation [6]. The specific emission topology of the cyclotron-maser instability therefore has significant bearing on the propagation characteristics and potential escape mechanisms for the radiation [10].

Experiments and simulations carried out at the University of Strathclyde [8-17] have investigated the electrodynamics of the cyclotron-maser instability driven by a magnetically compressed electron beam exhibiting a pitch-expanded horseshoe distribution in velocity

space. In the initial scaled laboratory experiments, the electron beam was injected from an annular explosive emission cathode and subject to significant magnetic compression using a highly configurable solenoid arrangement. The beam transport characteristics and cyclotron-resonant beam-wave coupling were simulated in 2.5D using the PiC code KARAT. Magnetic compression factors of up to $B_z/B_{z0} = 30$ were investigated with a 20cm long peak-plateau region for cyclotron-resonant beam-wave coupling. Within both the waveguide bounded simulations and experiments, cyclotron resonant energy transfer was studied with near-cutoff Transverse Electric (TE) modes, which closely match the electromagnetic field polarization of the X-mode with respect to the magnetostatic field. Although radiation propagation and coupling was assumed to be in the forward-wave direction (with respect to the cathode), a significant number of cyclotron-wave detunings resulted in backward-wave coupling. An example of such a regime is presented in figure 1, where a contour plot of E_θ from a 2.5D PiC simulation shows a more prominent backward-wave character to the cyclotron-wave coupling.

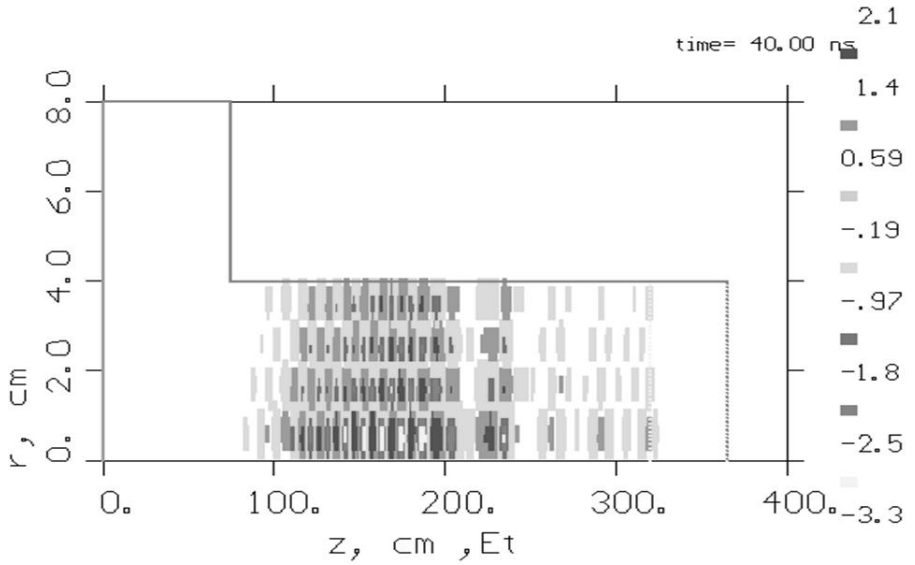

Fig. 1. Contour plot of E_θ within the waveguide-bounded simulation geometry.

In order to bridge between the waveguide-bounded experiments and an unbounded astrophysical scenario, we conducted PiC simulations to study the horseshoe driven cyclotron-maser instability in the absence of radiation boundaries. A 20keV, 14A electron beam was injected into a uniform axial magnetic flux density of 0.1T having a predefined horseshoe distribution, comprising a pitch spread of $\alpha = v_\perp / v_z = 0 \rightarrow 9.5$. Electromagnetically absorbent boundaries fully enclosed the simulated region to mitigate reflection and facilitate unconstrained emission.

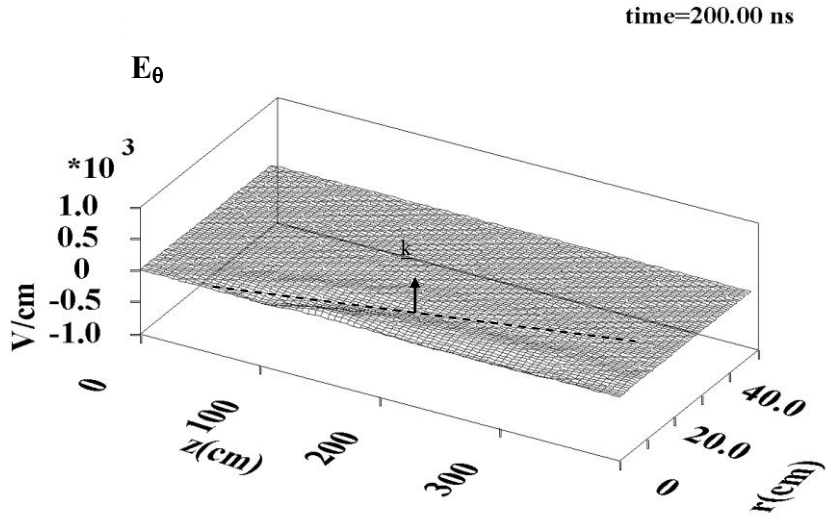

Fig. 2. 3D contour plot of E_θ within the unbounded simulation geometry.

The simulations demonstrate a clear relaxation of the electron horseshoe distribution via the cyclotron maser instability, with RF output generated in the X-mode at the electron cyclotron frequency with a small negative axial wavenumber. This is evidenced by the oblique propagation angle of the highlighted wave front presented in figure 2, which (factoring in the differing spatial scales of the *z* and *r* axes) corresponds to a backward-wave propagation angle of a few degrees.

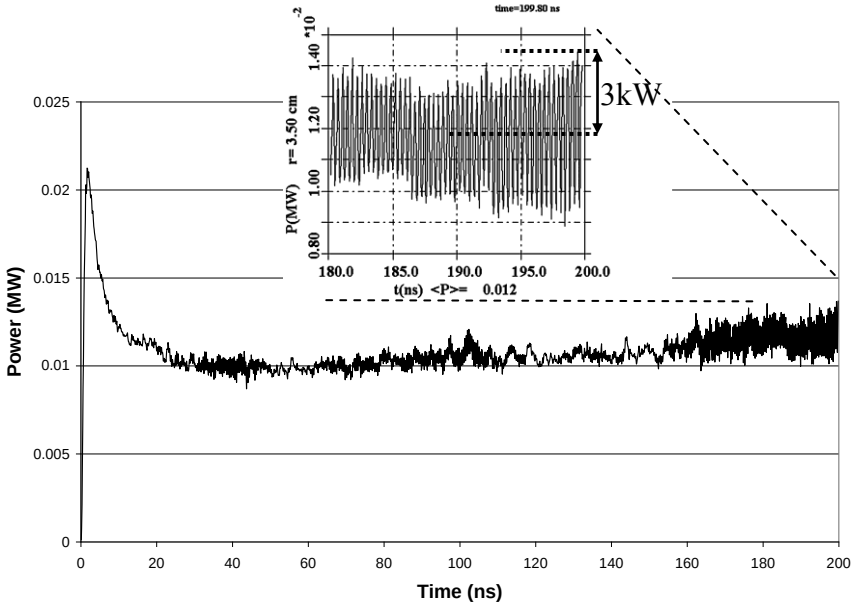

Fig. 3. Radial Poynting flux temporal evolution, measured in a plane at r = 3.5cm spanning the length of the simulation

A plot of the corresponding radial Poynting flux is presented in figure 3 measured in a plane at r = 3.5cm. A DC offset is present in the measurement due to low frequency EM field components associated with the electron beam propagation. After 180ns, a peak rf output power of ~3kW was measured corresponding to an rf conversion efficiency of 1.1% - comparable to the estimate of ~1% for the astrophysical phenomena [1].

In conclusion, PiC simulations have been conducted to investigate the electrodynamics and directional coupling of the cyclotron-maser instability attributed to numerous astrophysical radio sources [1-9]. Waveguide bounded computations demonstrate a well-defined cyclotron emission process, with a tendency to couple with finite negative $k_{\|}$. Similarly, unbounded simulations show RF output having a small negative axial wavenumber corresponding to a backward wave angle of a few degrees – consistent with minimum estimates required for a model of upward refraction and field aligned beaming of the radiation [10]. The corresponding RF conversion efficiency of 1.1% is comparable to earlier waveguide bounded simulations [14-17] and consistent with estimates of ~1% for the astrophysical phenomena [1].

References

[1] Treumann R.A., Astron. Astrophys. Rev., **13**, pp229-315, 2006.
[2] P. Zarka, Advances in Space Research, **12**, p99, 1992.
[3] Bingham R. and Cairns R.A., Physics of Plasmas, **7**, p3089, 2000.
[4] R. E. Ergun et al., Astrophys. J., **538**, pp456-466, 2000.
[5] P. L. Pritchett et al., J. Geophys. Res., **107**, p. 1437, 2002.
[6] R. A. Cairns et al., Phys. Rev. Lett., **101**, 215003, 2008.
[7] B. J. Kellett et al., Mon. Not. R. Astron. Soc., **329**, pp102-108, 2002.
[8] K. K. Lo et al., Mon. Not. R. Astron. Soc., **421**, pp3316-3324, 2012.
[9] M.C. Begelman et al., ApJ, **625**, pp51-59, 2005.
[10] J. D. Menietti et al., J. Geophys. Res., **116**, A12219, 2011.
[14] D. C. Speirs et al., J. Plasma Phys., **71**, pp665-674, 2005.
[15] S. L. McConville et al., Plasma Phys. Control. Fusion, **50**, 074010, 2008.
[16] K. Ronald et al., Plasma Sources Sci. Technol., **17**, 035011, 2008.
[17] K. Ronald et al., Plasma Phys. Control. Fusion, **53**, 074015, 2011.